

A Probe for in situ Detection of Defects in Buried Plastic Natural Gas Pipelines Remotely

James L. Spenik^{b*}, Christopher M. Condon^b, Mahendra P. Mathur^a, William L. Fincham^c

^a National Energy Technology Laboratory, 626 Cochran Mill Road, PO Box 10940, Pittsburgh, PA 15236-0940

^b REM Engineering Services PLLC, 3537 Collins Ferry Road, Morgantown WV, 26505

^c Parsons, 3610 Collins Ferry Road, P.O. Box 880, Morgantown, WV 26507-0880

Abstract

Several techniques are available to determine the integrity of a metal pipeline but very little is available in the literature to determine the integrity of plastic pipelines. It is known that since the decade of the 1970's much of the newly installed gas distribution and transmission lines in the United States are made out of polyethylene or some other plastic. This paper describes a method to determine the in-situ integrity of plastic natural gas pipelines.

A sensor based on capacitance technique has been developed at the National Energy Technology Laboratory. This sensor can be installed on a traversing probe to detect abnormalities in the walls of the plastic natural gas pipeline from the interior. This probe has its own internal power source and can be deployed into existing natural gas supply lines. Utilizing the capacitance parameter, the probe inspects the pipe for flaws and records the data internally. The data can be retrieved later for analysis of pipeline integrity.

* Corresponding author Tel.: (304) 285 – 4294 E-mail address: Spenik@NETL.DOE.GOV

Introduction

Since the 1970's a large portion of gas distribution lines have been fabricated from polyethylene¹ (PE). Also, as of 1995, about one-third of the 1.5 million miles of gas distribution pipelines in this country was made from PE. A special investigative report issued by the NTSB² indicates that hundreds of thousands of miles of plastic pipe installed from the 1960's through the early 1980's may be vulnerable to a phenomenon called "brittle-like cracking". An explosion and fire in Waterloo, Iowa on October 17, 1994 in which six persons died and seven more injured was attributed to gas released from a plastic service that failed in a brittle-like manner. Brittle-like failures, as a national average, may represent the second most frequent failure mode for older plastic piping, exceeded only by excavation damage.

Brittle-like cracking is characterized by the appearance of cracks through the wall of pipe with no visible deformations. This type of failure was not considered during testing in the early years of plastic pipe use, only hoop stress was considered. When hoop stress was applied to pipe during laboratory testing the usual failure mode was a ductile fracture characterized by significant deformation. The long term hydrostatic strength of polyethylene pipe used for natural gas service was determined by subjecting pipe samples to various hoop stresses and noting the time to failure. A log-log plot of time vs hoop stress was created and then extrapolated to 100,000 hours. The hoop stress at this point represented the hydrodynamic strength. Only internal pressures were used as design criteria for plastic pipe, external loadings that could cause additional stresses were not considered. It was believed that these stresses would be relieved by local yielding because of plastic pipes expected ductile behavior. After the middle of the 1980's standards were changed and the phenomenon of brittle-like cracking was accounted for. Polyethylene pipe used in new services probably will not exhibit brittle-like cracking but hundreds of thousands of miles of existing pipe may.

A number of techniques exist in literature to determine the integrity of metallic pipelines for gas distribution and gas transmission, such as ultrasonic, eddy current and acoustic wave to name a few. However, no satisfactory technique exists in literature that determines the flaws and defects in plastic pipeline. In this paper we describe a technique based on capacitance measurements that can detect flaws in already buried plastic gas distribution pipelines. A probe has been designed that can be inserted into the natural gas pipelines to examine the spatial dielectric characteristics of the pipe walls. The probe employs a sensor that measures the capacitance (or permittivity) of the pipeline wall. Any variation in the permittivity of the wall indicates that the area of the pipe wall under scrutiny has a defect.

Probe head geometry

The capacitance (C) between two plates is a ratio between charge (Q) accumulated on the plates and the associated potential drop (V). If the distance between the plates of a parallel plate capacitor (Figure 1) is d , the electric field intensity (E) is given by the ratio V/d and by Gauss' law $E = Q/A\epsilon$.

If the capacitance of a parallel plate capacitor is C_0 when the region between the plates is evacuated and C when the region is filled with a dielectric substance, the capacity of the condenser is altered when a dielectric substance is introduced between the plates. The ratio (C/C_0) is found to be independent of the size and shape of the condenser, and is characteristic of the particular dielectric medium that is introduced between the plates. In fact, this ratio is defined as the dielectric *constant* of the medium and is written as k Equation 1. The permittivity of free space (ϵ_0) is 8.854×10^{-12} Farad/m, ϵ is the particular material permittivity.

$$C = \frac{Q}{V} = \frac{Q\epsilon}{Qd/A} = \frac{Q\epsilon_0}{Qd/kA} = \frac{kA\epsilon_0}{d} \quad (1)$$

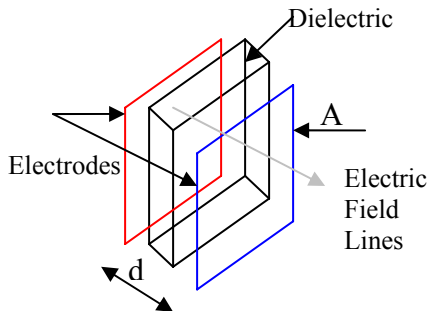


Figure 1 Parallel Plate Capacitor

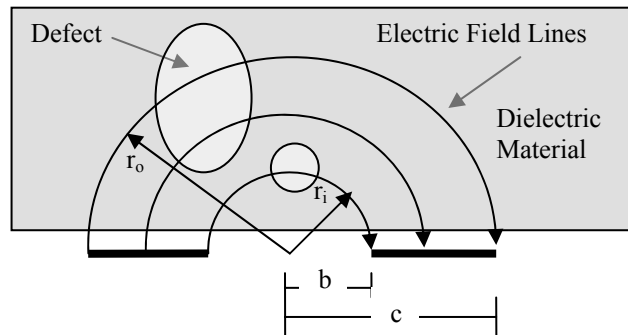


Figure 2 Opened parallel plate capacitor

The capacitance of a parallel plate capacitor is easily solved by Equation 1 provided fringing on the sides of the electrodes is ignored. In our case, since the probe will be entirely within the interior of the plastic pipe both of the capacitor plates will also be on the same side of the plastic pipe material to be tested. One configuration is a coplanar arrangement which allows the electric field to extend from one plate, through the material in question, to the other plate (Figure 2). This changes the operation of the capacitor into one with only a fringing field and thus Equation 1 is no longer valid³. For equal sized electrodes the electric field follows a circular arc, the minimum penetration distance of the electric field (r_i) is equal to half the distance between the inner edges of the two electrodes (b). The maximum penetration (r_o) is half the distance between the outer edges of the electrodes (c). This arrangement is used in common products such as “stud finders”⁴ but is inadequate for detection of defects within the walls of plastic pipes. Stray capacitances caused by wires in the electric circuit and other nearby conductive surfaces contribute noise above the required precision to detect abnormalities in a plastic pipe.

The problem of stray capacitance is solved by using a third coplanar electrode (guard) in the probe head^{5,6}. The guard is driven by a separate circuit which mimics the voltage variations of the driven electrode. The guard surrounds the driven electrode shielding it from stray capacitances as shown in Figure 3. The penetration depth of the probe can be calculated by examining the path of the electric field lines emanating from the edges of the electrodes. Using the complex solution, the field lines are circular arcs with radii described by Equation 2⁵. Rotating the circular arcs about the centerline creates a volume that is bounded by two semi-toroidal surfaces representing the measuring volume in cubic centimeters (Equation 3) where $R_0 = 0.5c$ and $R_i = a + 0.5(b - a)$. The total capacitance between the ground and driven electrodes can be derived from the complex potential field of a two-dimensional conformal mapping solution (Equation 4)⁵ where N is the geometric probe constant.

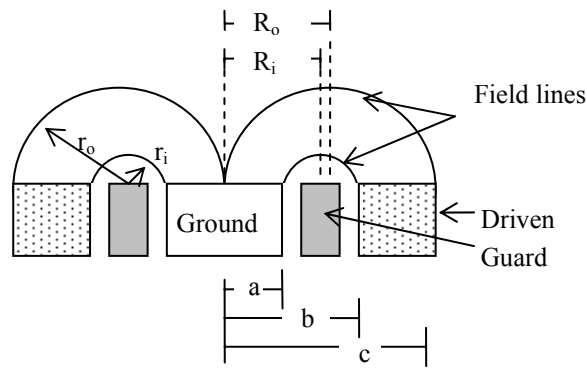


Figure 3 Capacitance probe with guard

$$r_o = (c^2 - a^2)/2c \quad \text{and} \quad r_i = (b^2 - a^2)/2b \quad (2)$$

$$Vol = \pi^2 (R_o r_o^2 - R_i r_i^2) / 1000 \quad (3)$$

$$C = 2a\epsilon \ln \left(\frac{c^2 - a^2}{b^2 - a^2} \right) = N\epsilon \quad (4)$$

The selection of the proper electrode diameters for a particular situation can be accomplished by normalizing Equations 2 and 3. By letting $K_1 = a/b$ and $K_2 = a/c$ Equations 2 and 3 become:

$$r_o/c = r_{oc} = (1 - K_1^2)/2 \quad (5)$$

$$r_i/b = r_{ib} = (1 - K_2^2)/2 \quad (6)$$

The maximum and minimum penetration depths with respect to dimension “a” become:

$$r_{oa} = \frac{r_o}{a} = r_{oc} \left(\frac{c}{a} \right) = (1 - K_1^2) / (2K_2) \quad (7)$$

$$r_{ia} = \frac{r_i}{a} = r_{ib} \left(\frac{b}{a} \right) = (1 - K_2^2) / (2K_1) \quad (8)$$

If the desired penetration depths are known the required ratios of electrode dimensions with respect to dimension “a” can be obtained from Figure 4

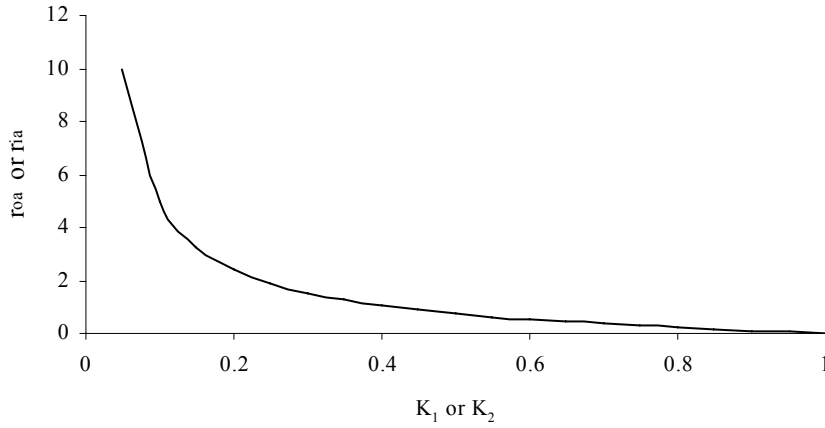


Figure 4 Normalized electrode ratios per unit penetration depth

Normalizing Equation 4 with respect to dimension a:

$$C_a = 2\epsilon \ln \left(\frac{K_2^2 (1 - K_1^2)}{K_1^2 (1 - K_2^2)} \right) \quad (9)$$

The capacitance (fF) of a generic probe head of this configuration in air normalized per mm radius of center electrode and combination of electrode parameters is shown on Figure 5.

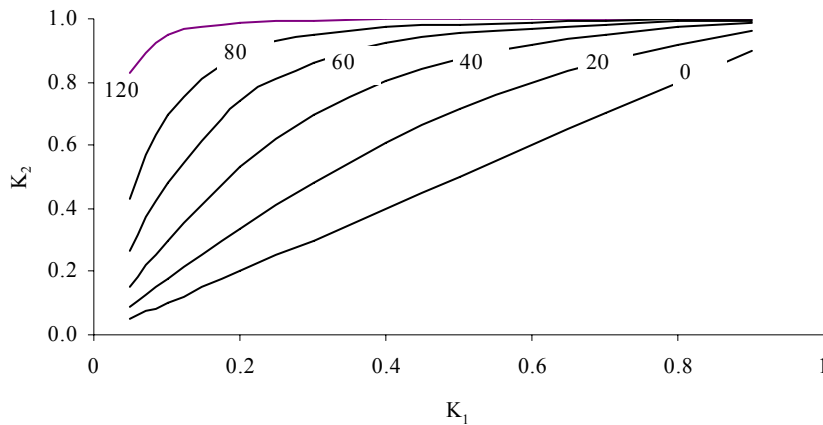


Figure 5 Normalized Capacitance (C_a) in fF/mm in air for combination of dimension ratios

The selection of the proper probe geometry is dependent upon the application. Maximum and minimum penetration depth must be considered as well as the ability to detect changes in permittivity within the measuring volume as a function of capacitance.

Initial Experiments

Preliminary experiments were conducted using commercially available equipment that had a primary function of non-contact displacement measurement to demonstrate the viability of the capacitance technique to locate voids in dielectric materials. A Capacitec clock drive (4100c), amplifier (4100-S1-BNC), and probe (HBC-75) were used. The electrode configuration of the probe is approximately that shown in Figure 6 with dimensions of: $a = 2.4$, $b = 2.8$ and $c = 4.8$ mm. According to Equation 2 the maximum penetration depth (r_o) should be approximately 1.8 mm, the minimum penetration depth (r_i) should be 0.4 mm (assuming the center guard electrode is small). The measuring volume was calculated to be approximately 0.07 cc and $k = 10.08$ mm. Clearly this probe was insufficient to identify defects within a pipe wall but should resolve surface defects.

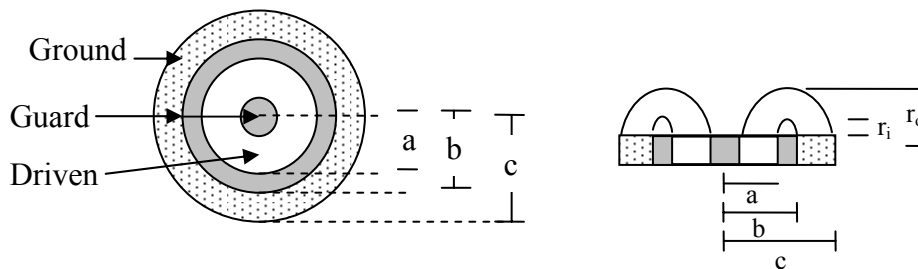


Figure 6 Electrode configuration of Capacitec HBC-75 probe

A section of 0.15 m diameter, 0.3 m long, polyethylene pipe was split in half and a series of defects were inscribed into the interior (Figure 7). A sampling region filled

with polyethylene would have a capacitance of 89 fF, devoid of polyethylene, 202 fF. Two 3.2 mm deep grooves 4.8 and 6.4 mm wide were cut into the top section. Rectangular defects were 25.4 mm long. The top rectangles were 4.8 wide, the bottom 0.64 cm. The depths (from left to right) of the defects ranged from 0.16 to 6.4 mm in 1.6 mm increments. The holes were 4.8 and 6.4 mm diameter with the same depth pattern as the rectangular defects. The probe was passed over the interior surface of the pipe in the longitudinal direction in steps of 0.8 mm for a total of 350 steps. The probe was returned to the original position then moved circumferentially 4.8 mm and another longitudinal sweep was conducted for a total of 37 sweeps. The data for each point, in the form of voltage, was placed in an array in accordance with its axial and circumferential position. A grayscale representation was produced which indicates the position of each of the defects (Figure 7). Figure 8 shows the results when the probe is retreated from the surface of a solid acrylic specimen. The normalized probe output reaches approximately 80% of maximum at the computed r_0 value of 1.8 mm.

This experiment demonstrated the ability of the capacitance technique to identify material property changes. However, due to the limited penetration depth this equipment is inadequate to identify defects in the interior of pipe walls. Also, this equipment consisted of bulky equipment and a power supply which required access to 120 vac. This type of arrangement is not suitable for in situ inspection of natural gas pipe thus a more suitable electronic package was required.

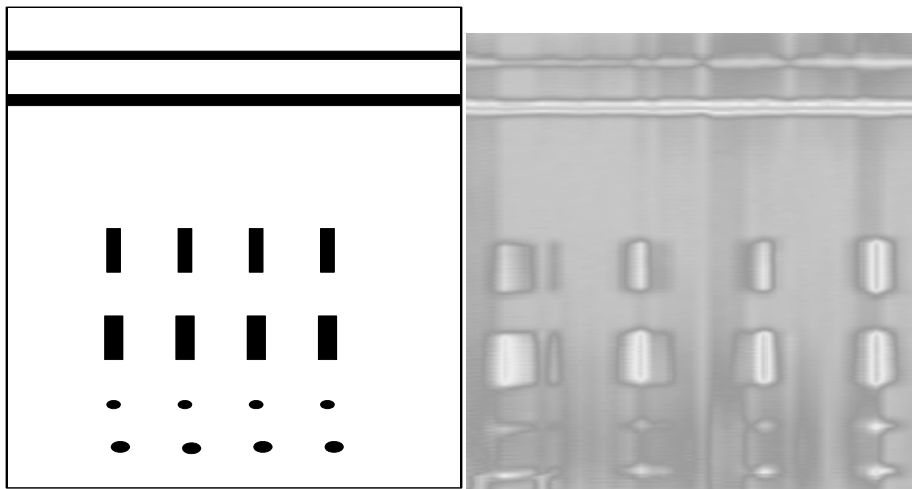


Figure 7 Position and image of defects

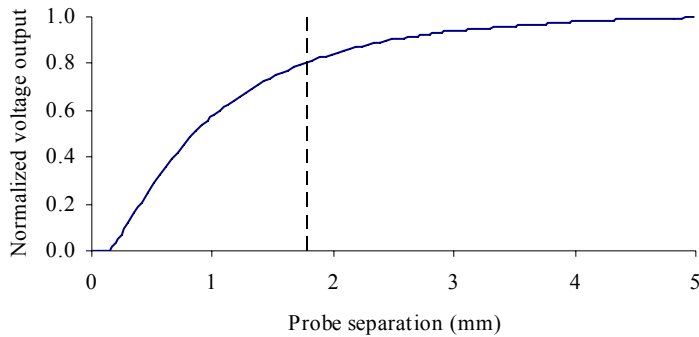


Figure 8 Normalized output as commercially available probe recedes from acrylic sample

Compact electronics package #1

Capacitance has traditionally been determined by variations in the time constant of RC circuits where the probe represents the capacitance portion. As the capacitor (probe) was charged the current flow approached zero asymptotically. In some cases a known RC combination was simultaneously charged and the charging rates were compared. The difference in charging rates allowed the probe capacitance to be deduced. Variations in this technique are used in the electronics for “stud finders”⁴ and in capacitance based proximity detectors⁷.

A first generation capacitance probe package was developed using this principle. The package required only a small number of components with power supplied from a 9 volt battery. The package was designed with an integrated programmable computer processor to control probe functions, measurements, and perform communication functions. This topology was chosen to eliminate the requirement for complicated equipment needed to drive guarded capacitive sense cables. Accuracy is enhanced by taking the measurement directly at the sensor circuit. The package incorporated a high-speed programmable microcontroller that measured the frequency of a capacitive oscillator using a quartz crystal timebase. The capacitive plates of the probe head were driven by a Maxim 7555 CMOS timer configured as a square wave oscillator with a resistive/capacitive time constant. A TL082 operational amplifier is used to duplicate the signal between the driven and ground electrodes to supply a signal to the guard electrode as shown in Figure 9. A PIC 16F88 microcontroller was used to institute a one second gate time to count the probe frequency and send the data to a host PC via serial port. The circuitry required a 5 volt power supply which was derived from the 9 volt battery through a 78L05 power regulator. The output of this configuration is in terms of frequency. As the permittivity of the material in the active region of the probe decreases the frequency output increases. A void within the region of influence will cause an increase in frequency.

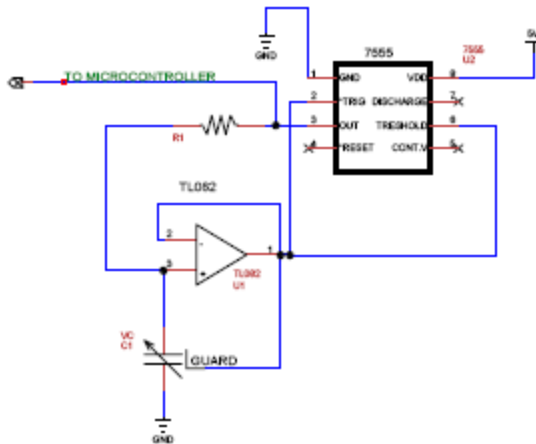


Figure 9 Sensor drive circuitry

The probe head used with this package had a somewhat different arrangement than the one previously described, stacked solid disks formed the electrodes (Figure 10) with dimensions of: $a = 4.3$, $b = 7.2$, $c = 12.8$, $r_o = 5.7$ mm, $r_i = 2.3$ mm and a measuring volume of 1.73 cc, the probe constant $k = 12.52$. The measuring volume is approximately 24 times that of the Capacitec probe, however, the probe constant increased by only 24% that of the Capacitec probe.

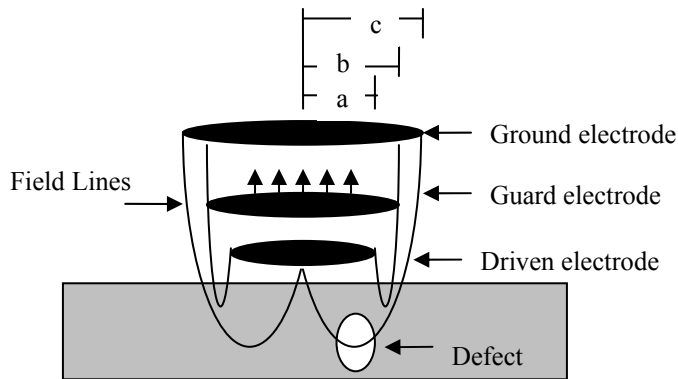


Figure 10 Capacitance probe head with stacked electrode configuration

A series of tests were conducted using acrylic. Polyethylene was replaced with acrylic for convenience in place of polyethylene. The dielectric constants of polyethylene $(2.26)^9$ and acrylic $(3.00)^9$, are similar. Since the goal was the detection a region with a dielectric constant of 1 the difference in dielectric constants between acrylic and polyethylene was not critical. With no material within the measuring volume the capacitance of the probe was calculated to be 111 fF, with all acrylic, 333 fF. The probe was passed over a 19 mm thick sheet of acrylic in which 6.1 and 4.6 mm diameter holes were drilled (Figure 11). The holes were drilled so 3 mm of residual material remained between the probe and the bottom of the hole. Assuming a 5.7 mm penetration depth when the probe detected each of the holes through the 3mm of residual material

Figure 12 shows the raw frequency output when the probe is passed over the both the front and back sides of the holes. The probe easily identifies the holes from the front side but the back side holes cannot be located using this format. When the outputs are normalized (Figure 13) the location of the 6.1 mm hole through the 3 mm of residual material becomes apparent, the 4.6 mm hole less so. However an upward trend of frequency with distance in the x direction, most likely due to increased separation in the y direction, makes this measurement less pronounced. The linear portion of output vs probe spacing in the y direction increases from 1 mm to 2 mm in this configuration but was somewhat less than the 5.7 mm predicted by Equation 2. This discrepancy may be due to the use of 1 mm thick polystyrene spacers between the plates used to provide electrical insulation. However, the ninety-eight percent limit was not reached until 9 mm of separation. A minimum separation distance was not observed, the output indicated a linear response from 0 to 2 mm of separation. The linear portion was over twice that of the previous configuration but still insufficient to resolve expected defects in plastic gas transmission or distribution lines.

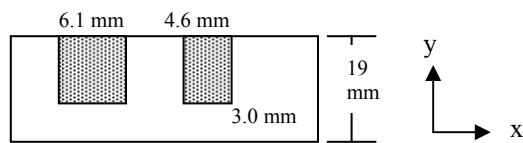


Figure 11 Position of holes in acrylic sample

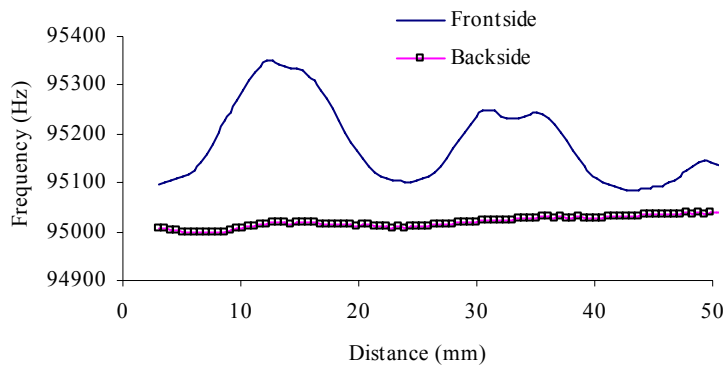


Figure 12 Probe traverse of 6.1 and 4.6 mm holes (raw frequencies)

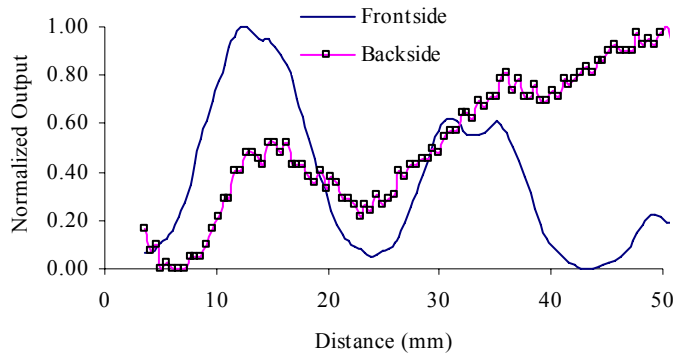


Figure 13 Probe traverse of 6.1 and 4.6 mm holes (normalized frequencies)

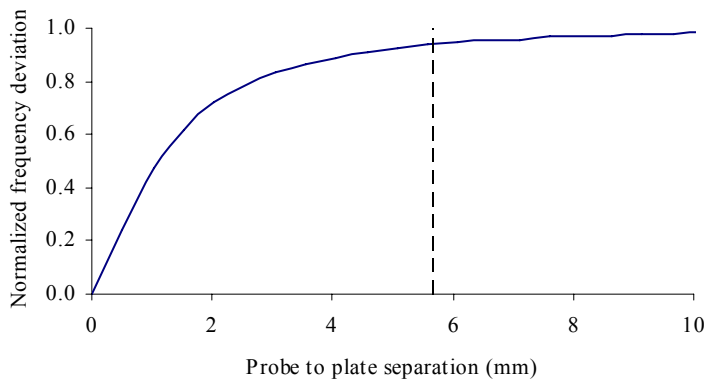


Figure 14 Normalized output as Generation 1 probe moves away from acrylic sample

The criterion for the second generation probe was the ability to detect a quarter inch hole through a quarter inch of material with the goal in mind that later refinements of the probe will have the ability to detect brittle-cracking. Since Equation 1 did not appear to be reliable in determining penetration depth, the 3D electromagnetic-field simulation package Ansoft's Maxwell[®] 3D was used to determine the optimum size of each electrode in the probe head. The size ratios between ground, guard and driven electrodes that would achieve the desired milestone were determined by examining variations in the electric field intensity. The optimum ratio was found to be 1 : 0.75 : 0.6. A diameter of 25.4 mm was selected for the ground electrode thus: $a = 7.6$, $b = 9.5$ and $c = 12.7$ mm. Using Equation 1 the minimum and maximum penetration depths were calculated to be 1.7 and 4.1 mm respectively. Electrodes on the probe head were separated using a thin layer of acrylic.

Compact electronics package #2

The circuitry for the second generation probe was redesigned to enable the detection of capacitance changes of 4 aF (10^{-18} F). When the probe was retreated from a solid sample of acrylic (Figure 15), the minimum penetration depth and the maximum distance at which a linear response ceased corresponded with the results of Equation 2. The output

of the previous circuit design had a tendency to float with time where this design remained stable. This proprietary circuit design also allows for data to be transmitted in real time or stored on-board for later evaluation.

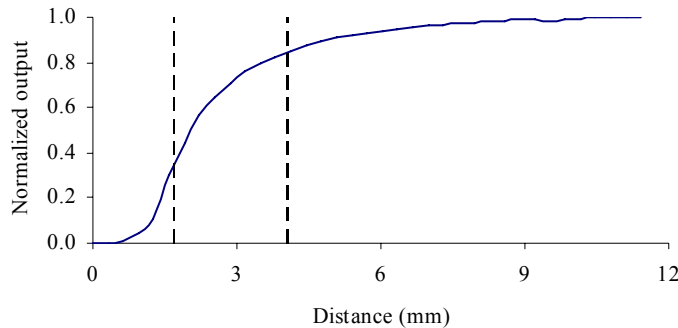


Figure 15 Normalized output as Generation 2 probe moves away from acrylic sample

Six 6.4 mm diameter holes with center to center spacing of 51 mm were drilled to various depths (0 – 11 mm) from the outside of a section of acrylic pipe 14.6 cm ID, 1.25 cm wall thickness. The second generation probe was passed through the inside of the pipe to determine its ability to detect the imperfections (Figure 16). The probe easily located the holes through 3.1 and 4.8 mm of residual material and marginally through 8.0 mm. Defects below 9.5 and 11 mm were not detected as expected.

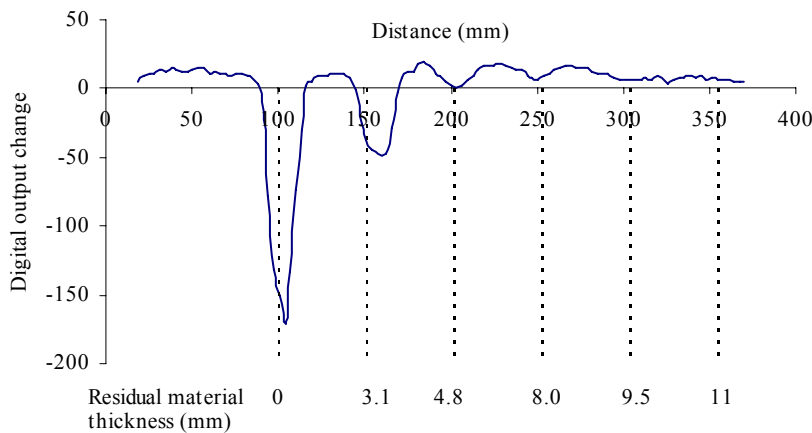


Figure 16 Third generation probe traverse of acrylic pipe

There are various sizes of plastic pipe used for natural gas transmission or distribution. A probe to detect defects in the walls of these pipes will need to be configured for each pipe diameter and wall thickness. Since the device operates by comparing the aggregate permittivity of material under the influence of an electrical field produced at the probe head, the ability to detect of a defect (volume with a different permittivity than the material) decreases as the overall material volume increases. The design of the probe

addressed in this paper assumes a nominal 152 mm (6 in) diameter polyethylene pipe with a wall thickness of 12.7 mm (0.5 in). The initial goal is to detect a 6.4 mm (0.25 in) diameter defect from the inside pipe wall. The defect begins on the exterior pipe wall and extends approximately half way through the wall (Figure. 17).



Figure. 17 Defect identification target (Battelle labs)

This technology was demonstrated at Battelle West Jefferson's Pipeline Simulation Facility near Columbus Ohio during the week of January 9th 2006⁸ for the Pipeline and Hazardous Materials Safety Administration (PHMSA) Pipeline Safety R&D program and DOE/NETL Gas Delivery Reliability Program. A test was conducted in which twelve defects of various sizes were placed in a 4 m length of 0.15 m diameter, 12.7 mm wall thickness, polyethylene pipe. Locations and characteristics of the defects were hidden from the experimenters and were not revealed until all data had been collected (Table 1). All defects were located at the same circumferential position. Defect depth ranged from 6.4 to 19.1 mm with volumes between 0.28 to 0.72 cc. Multiple scans of the specimen were conducted, Figure 18 is a representative example of those scans. The position of each defect, indicated by a decline in the value of the digital output, was accurately located using the in situ probe. The probe did not differentiate between the two identical defects (D15) but identified them as a single entity. The probe design exceeded the criteria of being able to locate a 6.4 mm diameter defect that begins 6.4 mm from the surface of the interior pipe wall.

Table 1 Characteristics of defects in polyethylene pipe

Defect #	Location (m)	Volume (cc)	Depth (mm)	Diameter (mm)	Comments
C1	0.457	0.46	6.4	9.5	Round defect
D1	0.635	0.72	10.2	9.5	Round defect
D2	-	-	-	-	No defect in region
D3	-	-	-	-	No defect in region
D4	1.168	0.36	11.4	6.4	Round defect
D5	1.346	0.41	5.1	3.2	Saw cut 25.4 mm long 3.2 mm wide
D6	-	-	-	-	No defect in region
D7	1.702	0.72	10.2	9.5	Round defect
D8	-	-	-	-	No defect in region
D9	-	-	-	-	No defect in region
D10	2.235	0.28	8.9	6.4	Round defect

D11				-	No defect in region
D12	2.591	0.66	8.9	3.2	Saw cut 22.9 mm long 3.2 mm wide
D13	2.769	0.66	2.3	19.1	Round defect
D14	2.946	0.25	3.6	9.5	Round defect
D15	3.124	0.28	8.9	6.4	2 identical holes 12.7 mm apart
	3.137	ea.	ea.	ea.	
D16	-	-	-	-	No defect in region
D17	-	-	-	-	No defect in region
D18	3.556	0.57	2.0	19.1	Round defect
D19	3.759	0.51	1.8	19.1	Round defect

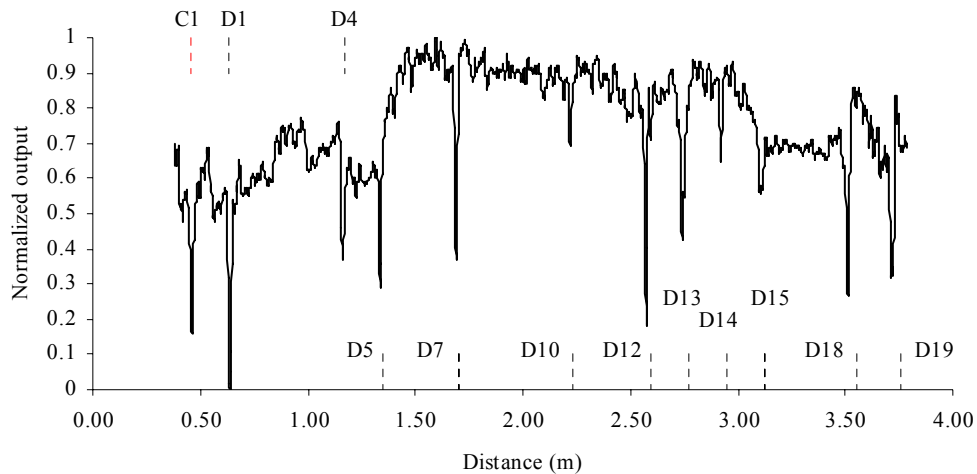


Figure 18 Probe output during transit of polyethylene pipe with intermittently spaced defects

Conclusions

A probe has been designed and tested that can detect defects existing on the outer wall of polyethylene pipe from the interior wall. The probe is self powered thus allowing the device to be placed in existing underground pipe and allowed to accumulate data concerning pipe integrity and then retrieved later for analysis. The current version of the probe only allows detection of defects along a single line but is currently being modified to allow detection of defects existing along the perimeter as well as an axial direction. Also, further modifications of the probe head design will allow flexibility in the types of defects that can be detected.

Nomenclature

- A – Area (mm²)
a - Center electrode outer radius (mm)
b - Outer electrode inner radius (mm)
C - Capacitance (Farad)
c - Outer electrode outer radius (mm)
d – Distance between parallel plates (mm)
E – Electric field intensity (volt/meter)
k - Dielectric constant
N – geometric probe constant = $2a \ln[(c^2 - a^2) / (b^2 - a^2)]$ (mm)
Q - Charge (Coloumb)
R_i – Major radius of inner electric field torus (mm)
r_i - Inner radius of electric field (mm)
R_o – Major radius of outer electric field torus (mm)
r_o - Outer radius of electric field (mm)
V - Voltage (Volt)
Vol – Measurement volume (cc)
ε - Permittivity of material (Farad/mm)
ε_o - Permittivity of free space (8.854 e⁻¹⁵ Farad/mm)

Bibliography

1. Mamoun, Michael M. Advances in PE pipe technology. Pipeline and Gas Journal. December 1995.
2. National Transportation Safety Board. Special Investigative Report. Brittle-like cracking in plastic pipe for gas service. NTSB/SIR-98/01. 1998
3. Mamishev, A. et al. Interdigital Sensors and Transducers. Proceedings of the IEEE. Vol. 92, No. 5. May 1992.
4. Franklin, Robert C., Fuller, Frank L., US Patent 4,099,118.
5. Acree Riley, C. , Louge, Michel. Quantative capacitance measurements of voidage in gas-solid flow. Particulate Science and Technology. Vol. 7, No 1-2, 1989.
6. Louge, M., Tuccio, M., Lander, E., Connors, P. Capacitance measurements of the volume fraction and velocity of dielectric solids near a grounded wall. Rev. Sci. Instrum. 67 (5) May 1996.
7. Vranish, J., McConnell, R. US Patent 5,166,679.
8. Pipeline and Hazardous Materials Safety Administration, Pipeline Inspection Technologies Demonstration Report, January 2006.
9. von Hippel, Arthur R., Dielectric Materials and Applications, The M.I.T. Press, Mass. Inst. Of Tech., Cambridge MA, 1954.